Experimental pK_a Values of Buried Residues: Analysis with Continuum Methods and Role of Water Penetration

Carolyn A. Fitch,* Daniel A. Karp,* Kelly K. Lee,* Wesley E. Stites,† Eaton E. Lattman,* and Bertrand García-Moreno E.*

*Department of Biophysics, The Johns Hopkins University, Baltimore, Maryland 21218 and †Department of Chemistry and Biochemistry, University of Arkansas, Fayetteville, Arkansas 72701 USA

ABSTRACT Lys-66 and Glu-66, buried in the hydrophobic interior of staphylococcal nuclease by mutagenesis, titrate with pK_a values of 5.7 and 8.8, respectively (Dwyer et al., 2000, *Biophys. J.* 79:1610–1620; García-Moreno E. et al., 1997, *Biophys. Chem.* 64:211–224). Continuum calculations with static structures reproduced the pK_a values when the protein interior was treated with a dielectric constant (ϵ_{in}) of 10. This high apparent polarizability can be rationalized in the case of Glu-66 in terms of internal water molecules, visible in crystallographic structures, hydrogen bonded to Glu-66. The water molecules are absent in structures with Lys-66; the high polarizability cannot be reconciled with the hydrophobic environment surrounding Lys-66. Equilibrium thermodynamic experiments showed that the Lys-66 mutant remained folded and native-like after ionization of the buried lysine. The high polarizability must therefore reflect water penetration, minor local structural rearrangement, or both. When in pK_a calculations with continuum methods, the internal water molecules were treated explicitly, and allowed to relax in the field of the buried charged group, the pK_a values of buried residues were reproduced with ϵ_{in} in the range 4–5. The calculations show that internal waters can modulate pK_a values of buried residues effectively, and they support the hypothesis that the buried Lys-66 is in contact with internal waters even though these are not seen crystallographically. When only the one or two innermost water molecules were treated explicitly, ϵ_{in} of 5–7 reproduced the pK_a values. These values of $\epsilon_{in} > 4$ imply that some conformational reorganization occurs concomitant with the ionization of the buried groups.

INTRODUCTION

Ionizable residues buried in the interior of proteins play key functional roles in fundamental biochemical processes such as catalysis, H^+ and e^- transport, photo-activation, and redox reactions. Those buried at the interfaces between molecules modulate recognition specificity and binding affinity. Elucidation of the structural basis of biological function in these processes requires quantitative understanding of electrostatic contributions. This usually entails measurement of pK_a values or redox potentials, elucidation of their molecular determinants, understanding of the molecular mechanisms whereby buried charges are stabilized, and of the structural and dynamic response of proteins to the ionization of a buried residue. For reasons of size and complexity, these issues are difficult to study experimentally in proteins where buried ionizable residues are functionally important, such as bacteriorhodopsin, cytochrome *c* oxidase, or photosynthetic reaction centers. In systems such as these, structure-based electrostatic calculations are necessary to bridge the gap between structure, energy, and function.

Meaningful calculation of electrostatic energies and pK_a values of buried ionizable residues remains challenging. The problems stem from difficulties in capturing quantitatively the dielectric relaxation in the protein interior. Fully microscopic approaches are not yet accurate enough to allow quantitative calculations of pK_a values (Del Buono et al., 1994; Schutz and Warshel, 2001). Therefore, continuum methods in which some of the contributions to the dielectric relaxation of proteins are captured implicitly through the use of dielectric constants remain useful and desirable, as long as they are calibrated against experimental data.

Most previous experimental and computational studies of pK_a values and their determinants have focused on surface ionizable residues. These groups are not useful to calibrate continuum models because the self-energies of surface groups in proteins are comparable to those in water (Sham et al., 1998). Buried groups with substantial pK_a shifts offer considerably greater insight about the nature of dielectric relaxation in the protein interior. They are also useful as benchmarks for testing, calibrating, and improving computational methods (Schutz and Warshel, 2001). Unfortunately, progress has been hindered by the lack of experimental pK_a values of buried groups. To address this problem, systematic, experimental studies of buried ionizable groups are underway in this laboratory. The approach entails burial of ionizable residues by mutagenesis, measurement of pK_a values, determination of crystallographic structures to describe microenvironments of buried groups, assessment of the consequences of ionization of buried groups on stability and structure, and analysis with structure-based energy calculations (García-Moreno E. et al., 1997; Dwyer et al., 2000).

Submitted November 14, 2001 and accepted for publication January 22, 2002.

Address reprint requests to Bertrand García-Moreno E., Dept. of Biophysics, The Johns Hopkins University, Baltimore, MD 21218. Tel: 410-516-4497; Fax: 410-516-4118; E-mail: bertrand@jhu.edu.

0006-3495/02/06/3289/16 $2.00

Previously, we reported that, when Lys-66 and Glu-66 are buried in a hydrophobic pocket in the interior of staphylococcal nuclease (SNase) by substitution of Val-66, they titrate with pK_a values of 5.8 and 8.8, respectively (García-Moreno E. et al., 1997; Dwyer et al., 2000). The ΔpK_a of 4.6 and 4.3 relative to the average pK_a values of Lys and Glu in water are among the largest ΔpK_a ever measured experimentally. Analysis with a Born formalism showed that the ΔpK_a are energetically equivalent to the transfer of an ion from water to a medium with dielectric constant in the range 9–12. This high apparent polarizability in the interior of SNase was initially puzzling. In independent structures of two mutants with Lys-66, obtained under conditions of pH where the buried Lys is neutral, the ionizable moiety of Lys-66 is encased in an extremely hydrophobic environment, incompatible with such high apparent polarizability (Stites et al., 1991; García-Moreno E. et al., 1997). We conjectured initially that the high polarizability reported by Lys-66 reflected a substantial structural relaxation concomitant with the ionization of the buried Lys-66. However, in two subsequent structures with buried Glu-66, also obtained under conditions of pH where the buried Glu is neutral, internal water molecules were found interacting with the carboxyl group of Glu-66 and connecting it to bulk water (Dwyer et al., 2000). These structures suggested that the high apparent polarizability in the interior of SNase could reflect the presence of internal water molecules near the buried ionizable residues.

Many factors can contribute to the energetics of ionization of a buried group, and thus to the apparent polarizability reported by its pK_a: interactions with backbone and side chain dipoles, with ionizable residues, and with buried water molecules; changes in the state of ionization of other residues; and relaxation of the protein. One of the aims of this study is to dissect the dielectric response in the interior of SNase with a combined experimental and theoretical approach. Equilibrium thermodynamic and ^{1}H-NMR experiments were performed to ensure the accuracy of the pK_a of Lys-66, and to assess the consequences of the V66K mutation on the structure and stability of a hyperstable Δ+PHS nuclease variant. The experiments were also necessary to determine the consequences of the ionization of the buried Lys-66 on the structure of the Δ+PHS/V66K protein. Specifically, it was important to establish that this protein remained folded and native-like after ionization of the buried group. This information was needed to understand the meaning of the high polarizability reported by the buried ionizable group, and to ensure that it did not simply reflect a large structural transition such as acid denaturation. Electrostatic interactions between buried and surface ionizable groups were also assessed experimentally to determine their effect on the pK_a values of the buried groups.

The study has three computational aims. First, to quantitate the influence of the buried water molecules on the pK_a value of Glu-66 by comparing different structure-based pK_a calculations, some of which omitted the internal water molecules, others which treated them explicitly. Second, to test the hypothesis that the buried ionizable moiety of Lys-66 is also in contact with internal water molecules that are either disordered or only transiently buried, and thus crystallographically invisible. Third, to use the experimental pK_a of Glu-66 and Lys-66 to determine the empirical values of the dielectric constants in the protein interior useful for structure-based calculations of pK_a values of buried residues. These studies underscore the important contributions from water penetration to pK_a values of buried groups, and they contribute insight about mechanisms of dielectric relaxation in the interior of SNase.

MATERIALS AND METHODS

Staphylococcal nuclease

The hyperstable Δ+PHS variant of nuclease includes mutations P117G, H124L, S128A, G50F, V51N, and a deletion from residues 44–49. Clones of Δ+PHS nuclease and its V66K mutant, Δ+PHS/V66K, were obtained from Prof. David Shortle (The Johns Hopkins University). Protein was expressed and purified following the method of Shortle and Meeker (1986). The protein was determined to be >98% pure by SDS-PAGE. The concentration was determined using an extinction coefficient of 15,600 $M^{-1}cm^{-1}$ at 280 nm.

Equilibrium thermodynamic measurements

The protocols that were used for measurement of stability by GdnHCl-denaturation monitored by the intrinsic fluorescence of Trp-140 have been described previously (García-Moreno E. et al., 1997; Dwyer et al., 2000; Whitten and García-Moreno E., 2000). The unfolding of Δ+PHS nuclease and of some of its mutants by chemical denaturants is considerably slower than for wild-type SNase. In the automated denaturation experiments, samples were allowed to equilibrate for 40–80 min between the addition of denaturant in the transition region. Five minutes were sufficient to reach equilibrium in the baseline regions. The following buffers were used at a concentration of 25 mM to cover the pH range specified: Acetate, pH 4 to 5.5; MES, 5.5–6.5; HEPES, 7–8; TAPS, 8–9; CHES, 9–10; CAPS, 10–11. The experiments were performed with an ATF-105 automated titration fluorometer from Aviv Inc. (Lakeland, NJ). All data were collected at 25°C, 100 mM NaCl.

Protocols for acid-base titrations monitored by fluorescence have also been described previously (Whitten and García-Moreno E., 2000). The only notable difference with experiments reported previously is that the acid-induced unfolding of Δ+PHS nuclease is also slower than that of wild type, and required equilibration times as long as 5 min between addition of titrant. All measurements were performed at 25°C, 100 mM NaCl, in a buffer consisting of 5 mM MES and 5 mM HEPES.

The measurement of proton (H^+) titration data with potentiometric methods has been described previously (Dwyer et al., 2000; Whitten and García-Moreno E., 2000). The data in this paper are measured with concentrations of SNase of 3–4 mg/ml. Reversibility of the titration curves was tested routinely to ensure that the system was at equilibrium. All titration curves were measured in triplicate. All measurements were performed at 25°C, 100 mM KCl or in 6 M GdnHCl and 100 mM KCl.

Measurement of pK_a values by ^{1}H-NMR spectroscopy

The procedures of Lecomte and co-workers were used to determine pK_a values by NMR spectroscopy (Lecomte and Cocco, 1990; Cocco et al., 1992; Bhattacharya and Lecomte, 1997; Kao et al., 2000). Protein samples at concentrations of ~1.2 mM were prepared by solvent exchange in D_2O containing 100 mM KCl. Amide hydrogen atoms were exchanged by increasing the temperature to the midpoint temperature for 15 min followed by centrifugation. A total volume of at least 1.2 ml was prepared at pH 8.0, and this sample was split into two fractions, one for titration with acid and one for titration with base.

One-dimensional (1D) ^{1}H-NMR spectra were acquired at 25°C on a Varian Unity Plus 500 MHz spectrometer using a 5-mm triple-resonance probe. Spectra were recorded with low-power water presaturation. A 90° high-power pulse (8 μs) was applied followed by acquisition of 16-K data points with a sweep width of 6024 Hz. Each spectrum contains 256 transients. All spectra were referenced to the chemical shift of the residual HDO line, which in turn was referenced to the external reference sodium 2,2-dimethyl-2-silapentane-5-sulfonate (Wishart et al., 1995). Spectra were recorded at 25°C. The temperature was calibrated based on measurements of the temperature-dependent change in chemical shift of the C and OH group of ethylene glycol (Martin et al., 1980). Temperatures were calibrated to ±1°C and maintained to ±0.1 for both spectral acquisition and pH measurements.

Values of pH during the titration were measured with a combination pH electrode (Ingold 6030−02, Mettler-Toledo, Columbus, OH) and a Radiometer PHM 95-pH meter (Radiometer Analytical, Lyon, France). Measurements were made before and after data acquisition, with the latter value being assigned to the spectra. Estimated errors in pH measurements are 0.10. Uncorrected pH meter readings are reported based on the assumption that the electrode isotope effect is canceled by the isotope effect on the histidinium (Glasoe and Long, 1960; Li et al., 1961). Titrations were carried out with NaOD and DCl (Isotec, Miamisburg, OH). HDO saturation was complete for the ppm range of interest. Cϵ^1H signals from each of the four histidine residues were assigned unambiguously in 1D spectra of wild-type SNase (Alexandrescu et al., 1988).

The Cϵ^1H resonances obtained from 1D ^{1}H-NMR were used to monitor the ionization of individual histidines because they are shifted far down field, they are well resolved, and their chemical shift is quite sensitive to the local environment. Multiple resonances are observed for histidines in SNase (Alexandrescu et al., 1989). The dominant resonance is thought to be due to the *cis* form of the peptide bond between Lys-116 and Pro-117 (Evans et al., 1989). This is also the crystallographically observed configuration of this bond (Loll and Lattman, 1989; Hynes and Fox, 1991. Minor resonances are attributed to the *trans* conformation. An additional minor resonance has been identified at high concentrations. This form is concentration dependent, thus it is attributed to a dimeric form or higher order aggregate of SNase (Alexandrescu et al., 1989). It has been shown previously that the titration behavior of the minor resonances of a given histidine are similar (Fox et al., 1986; Alexandrescu et al., 1989. The pK_a values of histidines in SNase measured by ^{1}H-NMR spectroscopy are insensitive to protein concentration according to repeated experiments at concentrations ranging from 0.9 to 1.5 mM.

Analysis of 1D data sets was performed with Felix version 97.2 on a Silicon Graphics R10000 workstation. Time-domain data points were fast Fourier-transformed following zero filling and application of a soft sine bell window. Signal peaks were obtained from the Felix peak picking function. The pK_a values of the histidine Cϵ^1H signals were determined by nonlinear least squares fit with (Markley, 1975),

$$\delta(\mathrm{pH}) = \delta_0 + (\delta_+ - \delta_0)\frac{10^{n(pK_a - pH)}}{1 + 10^{n(pK_a - pH)}}. \qquad (1)$$

In this expression, δ_+ and δ_o refer to the value of the chemical shift (δ) in the acid and basic limits of the transition, and *n* is a phenomenological Hill coefficient. Error in the calculated pK_a values is estimated to be less than 0.07 based on three independent experiments.

pK_a calculations with semi-macroscopic continuum methods

The single-site ionization method described by Antosiewicz et al. (1994, 1996) was used for all calculations of electrostatic energies and pK_a values, with some modifications noted below. The University of Houston Brownian Dynamics package (Davis et al., 1991) was used to calculate electrostatic potentials by solution of the linearized form of the Poisson–Boltzmann equation by the method of finite differences. The cluster method of Gilson (1993) was used to calculate ionization energies and mean charges. Polar hydrogen atoms were added to the protein in the neutral state with the HBUILD facility in CHARMm (Accelrys Inc., www.accelrys.com). The position of the hydrogens was energy minimized with 500 steps of steepest descent with CHARMm version 25.3, performed while all heavy atoms were kept static. Hydrogen atoms were placed on OD2 of all Asp, and on the OE2 of all Glu. The tautomeric forms of His were selected from the best fit to the experimental pK_a values. This placed hydrogen atoms on Nϵ2 of His-8, on Nδ1 of His-46, on Nϵ2 of His-121, and on Nδ1 of His-124. Partial charges were taken from the CHARMm polar-hydrogen-only topology file version 21 (CHARMm, Accelrys Inc.; Neria et al., 1996) and atomic radii from the OPLS parameter set (Jorgensen and Tirado-Rives, 1988). The following set of model compound pK_a values was used in the calculations: C-term, 3.8; Asp Cγ, 4.0; Glu Cδ, 4.4; His Nδ1 or Nϵ2, 6.3; N-term, 7.5; Tyr OH, 9.6; Lys Nζ, 10.4; Arg Cζ, 12.0. In all the calculations, the temperature was 298 K, the Stern layer was set at 2.0 Å, the external dielectric constant was 78.5, and the protein dielectric constant, ϵ_{in}, was a variable. A Richard's probe-accessible surface was used with a probe radius of 1.4 Å.

The water molecules that were included explicitly in the calculations were treated as TIP3 waters (Jorgensen et al., 1983). Water hydrogen atoms were added with HBUILD. To explore the effects of water reorientation in response to ionization of the buried groups, the position of water hydrogen atoms was relaxed by minimization with the buried group in the charged state. All minimization procedures consisted of 500 steps of steepest descent with CHARMm v25.3. The minimization was carried out in two steps. In the first minimization step, all ionizable groups were kept in the neutral state except for the buried residue of interest, while the hydrogen atoms of protein polar atoms and of buried water molecules were minimized. In the second minimization step, the hydrogen atoms in protein polar atoms were allowed to relax while the buried ionizable residue was in the neutral state, and the water molecules were fixed in the positions that resulted from the first minimization. To investigate further the effects of water relaxation, additional conformations were obtained from minimization as described above, in which the water oxygen atoms were also allowed to reposition. The role of individual water molecules was explored in two ways. First, by progressively removing individual water molecules from an energy-minimized conformation and assessing the consequences in the calculated pK_a values. Second, by minimizing conformations after removal of individual water molecules, and then evaluating the consequences on the calculated pK_a values.

The calculations were performed with the structures of PHS/V66E and Δ+PHS/V66K determined previously in this laboratory. The only water molecules that were treated explicitly in the calculations with SNase are the four water molecules that connect the buried Glu-66 with bulk water (Dwyer et al., 2000). To estimate the effects of buried water on the pK_a of Lys-66, position 66 in the PHS/V66E structure was mutated into a lysine with the InsightII software package (Accelrys Inc.). The resulting structure was energy minimized with a procedure that only allowed relaxation of Cγ to Nζ atoms of Lys-66 and of oxygen and hydrogen atoms of the four water molecules.

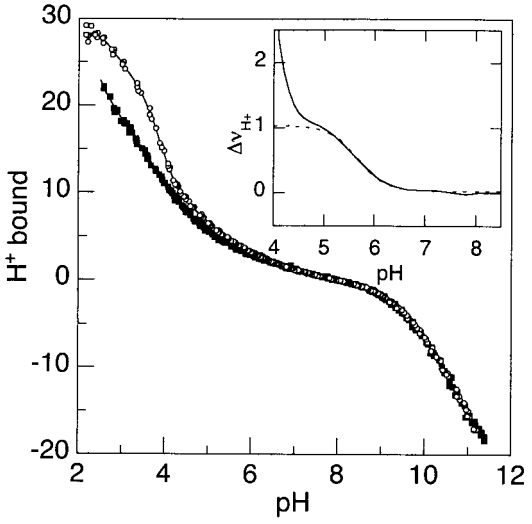

FIGURE 1 Potentiometric H^+ titration of Δ+PHS nuclease (*filled squares*) and its Δ+PHS/V66K mutant (*open circles*) in 100 mM KCl, 25°C. The solid lines through the experimental data represent fits with eighth-order polynomials. The insert includes the difference between these curves (*solid line*) and the fitted isotherm of a group with a pK_a of 5.7 (*dashed line*).

RESULTS AND DISCUSSION

pK_a value of the buried Lys-66

Previously, we reported a pK_a of 6.35 for Lys-66 in wild type SNase and in PHS nuclease, a hyperstable variant that is 3.4 kcal/mol more stable than the wild type (García-Moreno E. et al., 1997). The ionization of the buried Lys-66, even in the hyperstable PHS background, partially unfolds the protein. For this reason the pK_a of Lys-66 was re-examined in the Δ+PHS background, which, at 25°C, is 6.7 kcal/mol more stable than wild type. A preliminary pK_a of Lys-66 in Δ+PHS/V66K was published previously (García-Moreno E. et al., 1997). However, the pK_a values of these buried residues are measured by indirect thermodynamic methods rather than by a site-specific method based on NMR spectroscopy, thus it was essential to demonstrate that the pK_a value of Lys-66 in Δ+PHS/V66K was accurate. This was accomplished by measuring pK_a values by two completely independent equilibrium thermodynamic methods. First it was obtained from the difference in potentiometric H^+ titration of Δ+PHS nuclease and its V66K mutant (Δ+PHS/V66K). Then it was obtained by linkage analysis of the pH dependence of stability of these two proteins. These data were also necessary to assess the effects of the V66K mutation and of the ionization of the buried Lys-66 on the structure and stability of Δ+PHS/V66K.

The potentiometric H^+ titration curves of Δ+PHS and Δ+PHS/V66K are shown in Fig. 1. The two titration curves are superimposed arbitrarily at pH 9; the difference between them ($\Delta\nu_{H+}$) is shown in the insert. Between pH 6.5 and 11.5 the titration curves are identical. This demonstrates that the V66K mutation had no structural consequences that affected the pK_a values of surface groups that titrate in this pH range, where the buried Lys-66 is neutral. The two titration curves diverged at pH $<$ 6.5 because of the ionization of the buried Lys-66.

The pK_a of Lys-66 extracted by fitting a single-site isotherm to the $\Delta\nu_{H+}$ curve in Fig. 1 is 5.6 (5.52, 5.66). This pK_a is considerably lower than the normal pK_a of 10.4 of lysine in water (Matthew et al., 1985). It is also lower than the value of 6.38 measured previously in the wild type and in the PHS background (García-Moreno E. et al., 1997). The fit of the isotherm to the difference titration curve is excellent at pH $>$ 4.5. Below this pH value the isotherm does not fit the experimental data because the difference H^+ binding curve also reflects proton uptake concomitant with the acid unfolding of Δ+PHS/V66K.

The H^+ titration behavior of Δ+PHS/V66K was also measured potentiometrically under unfolding conditions (6 M GdnHCl) to assess further the ionization properties of Lys-66 and its effect on the global stability of Δ+PHS nuclease. The H^+ titration curves in native and denatured states are compared in Fig. 2 *A*. The distance between these two curves was determined explicitly with batch experiments, which measured the number of H^+ bound by SNase when GdnHCl was added to a solution of SNase in 100 mM KCl to a final concentration of 6 M. The difference (unfolded minus native) between these H^+ binding curves is shown in Fig. 2 *B*. This $\Delta\nu_{H+}$ curve has three notable features. First, the convergence toward $\Delta\nu_{H+} = 0$ above pH 9 shows that, in the unfolded state, Lys-66 ionized with a pK_a close to 10, in agreement with the known pK_a of 10.4 of lysine in water. Second, the value of $\Delta\nu_{H+} \approx 1$ between pH 9.5 and 6.3 shows that, in this pH range, there is one extra H^+ bound to the unfolded protein that is not bound to the folded protein. This is consistent with the difference between the $pK_a > 10$ for Lys-66 in the unfolded state, and the pK_a of 5.6 in the native state. Third, the drop in $\Delta\nu_{H+}$ toward 0 that occurred at pH $<$ 6.3 is consistent with the pK_a of 5.6 for Lys-66 in the native state obtained from the data in Fig. 1. The pK_a of Lys-66 in the native state could not be resolved from the $\Delta\nu_{H+}$ curve in Fig. 2 *B* because, below pH 5, preferential H^+ uptake by the GdnHCl-unfolded state relative to the native state masked the H^+ binding reaction of Lys-66.

The second method used to determine the pK_a of Lys-66 involved linkage analysis of the pH dependence of stability of Δ+PHS nuclease and the Δ+PHS/V66K mutant. The free energy differences between native and denatured SNase ($\Delta G^o_{H_2O}$) measured by GdnHCl denaturation monitored by fluorescence are shown in Fig. 3. Δ+PHS is more than twice as stable as wild-type SNase at neutral pH. The stability of Δ+PHS was not pH sensitive in the range 4.5–9.5, but it decreased at pH $<$ 4.5. In contrast, the stability of Δ+PHS/V66K decreased markedly between pH

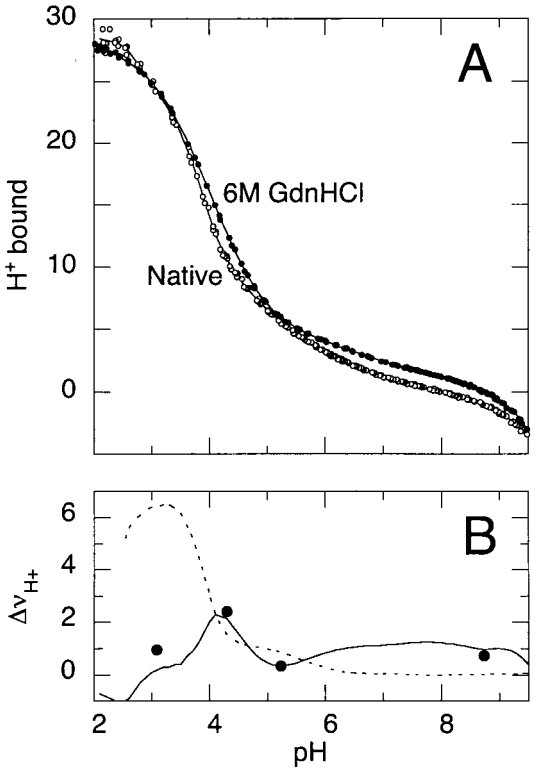

FIGURE 2 (*A*) Potentiometric H^+ titrations of Δ+PHS/V66K under native conditions (*open circles*) and in 6 M GdnHCl (*filled circles*) at 25°C. (*B*) Preferential H^+ binding of GdnHCl-denatured protein obtained as the difference in the continuous titration curves in (*A*) (*solid line*), and with batch experiments (*filled circles*). The $\Delta\nu_{H+}$ obtained by batch experiments represent the average of three independent experiments. The error is smaller than the diameter of the symbols. The difference in the H^+ titration curves in Fig. 1 is included for comparison (*dashed line*).

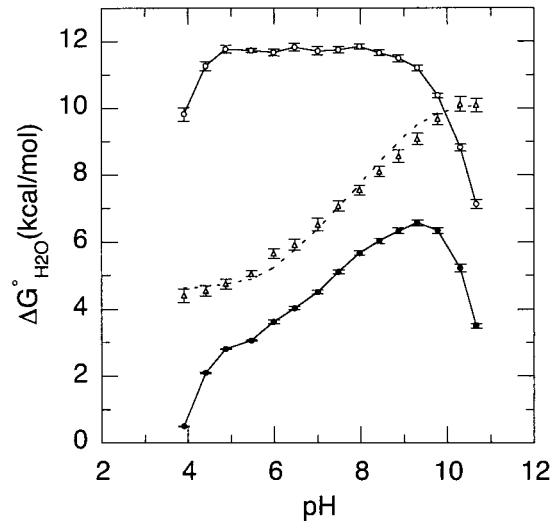

FIGURE 3 Stability of Δ+PHS (*open circles*) and Δ+PHS/V66K (*filled circles*) nuclease determined by fluorescence-monitored GdnHCl denaturation at 25°C. The solid lines through the data are only meant to guide the eye. The difference between these curves (*open triangles*) and the fit of Eq. 1 (*dashed line*) are shown. For display purposes the $\Delta\Delta G^o_{H_2O}$ curve was shifted along the ordinate; information about the pK_a of Lys-66 lies in the shape, not in the absolute magnitude of this curve.

9.5 and 4. According to the titration curves in Fig. 1, the H^+ binding properties of these two proteins were identical between pH 11.5 and 6.5. Therefore, the loss of stability of Δ+PHS/V66K in this range of pH must reflect the depressed pK_a of Lys-66 when it is buried in the hydrophobic core of the folded protein. The difference between the two stability curves ($\Delta\Delta G^o_{H_2O}$) is also shown in Fig. 3. In the linear region, the slope of the difference stability curve was 1.25 kcal/mol, close to the theoretical value of 1.36 kcal/mol, equivalent to $\Delta pK_a = 1$ at 25°C.

The pK_a values of Lys-66 in the native and unfolded states were obtained by fitting the $\Delta\Delta G^o_{H_2O}$ versus pH curve in Fig. 3 with (Stites et al., 1991)

$$\Delta\Delta G^o_{H_2O}(\mathrm{pH}) = \Delta\Delta G^o_{H_2O}(\mathrm{mut}) - RT \ln \frac{1 + e^{2.303(pK_a^D - \mathrm{pH})}}{1 + e^{2.303(pK_a^N - \mathrm{pH})}}. \quad (2)$$

The rightmost term describes the pH-dependent component of $\Delta\Delta G^o_{H_2O}$. The pH-independent term, $\Delta\Delta G^o_{H_2O}(\mathrm{mut})$, reflects the energetic consequences of the mutation other than the electrostatic effects related to shifts in pK_a values. Fitting with Eq. 2 yields a denatured state pK_a value (pK_a^D) of 9.76 (9.26, 10.32), slightly lower than the pK_a value of 10.4 in water (Matthew et al., 1985). The pK_a value in the native state (pK_a^N) is 5.76 (5.52, 5.96), in excellent agreement with the pK_a value that was determined potentiometrically.

Analysis of the $\Delta\nu_{H+}$ versus pH curve in Fig. 1 with a single-site H^+ binding isotherm, and of the $\Delta\Delta G^o_{H_2O}$ versus pH in Fig. 3 with Eq. 1, both assume that the V66K mutation does not affect the ionization properties of other groups. This assumption is validated by the data in Fig. 1, and by the slope of $\Delta\Delta G^o_{H_2O}$ versus pH in Fig. 3, which suggests that the dependence of stability on pH is determined primarily by the shift in the pK_a of a single group. The excellent agreement between pK_a values determined by independent thermodynamic methods also supports the validity of this assumption.

Ionization of the buried Lys-66 does not unfold nuclease

To understand the mechanisms of dielectric relaxation upon ionization of the buried groups, it is necessary to characterize the effects of the titration of the buried group on the conformation of the protein. Previously, it was demonstrated that PHS/V66D is mostly folded after ionization of the buried Glu-66 (Dwyer et al., 2000). However, the ionization of Lys-66 in the wild type and in PHS nuclease disrupts the native conformation and leads to measurable

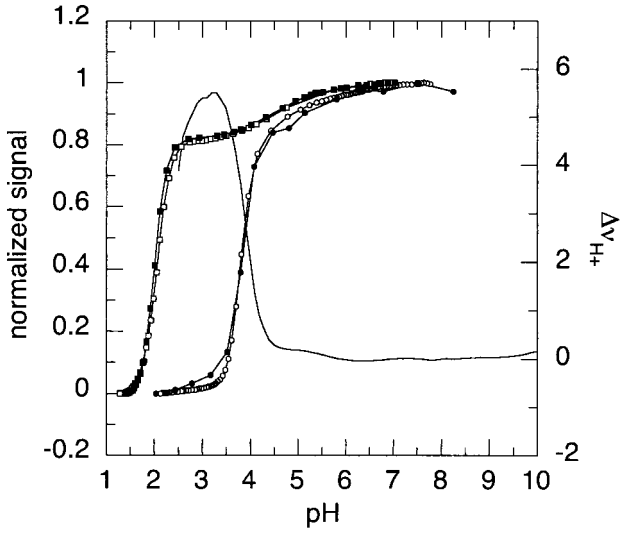

FIGURE 4 Acid/base titrations of Δ+PHS (*squares*) and Δ+PHS/V66K (*circles*) nuclease monitored by fluorescence (*filled symbols*) and far-ultraviolet CD (*open symbols*). The lines through the data are only meant to guide the eye. Superimposed, with reference to the right axis, is the difference H^+ binding curve from Fig. 1 (*thin line*) from which the titration of a group with a pK_a of 5.7 has been subtracted.

global or partial unfolding (Stites et al., 1991; García-Moreno E. et al., 1997). Thus, it is important to assess the conformational state of Δ+PHS/V66K SNase under conditions of pH where Lys-66 is charged.

Five thermodynamic and spectroscopic observations demonstrate conclusively that, in the hyperstable Δ+PHS background, the ionization of the buried Lys-66 does not unfold the protein or perturb its global conformation in a detectable manner.

1. The uptake of H^+ that signals the onset of acid denaturation occurs at pH < 4.2, more than 1 pH unit below the pK_a of 5.7 for Lys-66 (insert in Fig. 1). This is also evident in the ΔH^+ curve in the lower panel in Fig. 2. The increase in $\Delta\nu_{H+}$ at pH 5.1 and below reflects greater H^+ binding to Δ+PHS/V66K in 6 M GdnHCl than in 100 mM KCl. This implies that the pK_a values of the acid groups in Δ+PHS/V66K are still depressed and native-like after the ionization of the buried Lys-66. The maximum in the $\Delta\nu_{H+}$ curve near pH 4.2 identifies the pH at which the acid unfolding transition begins.
2. The stability of Δ+PHS/V66K is approximately 3 kcal/mol at the pH corresponding to the pK_a of Lys-66 (Fig. 3). Therefore, at this pH, the protein is predominantly in the native state. Even at pH 4.4, more than a pH unit below the pK_a of Lys-66, $\Delta G^o_{H_2O}$ is still greater than 2 kcal/mol. The steep change in $\Delta G^o_{H_2O}$ below this pH signals the onset of acid-denaturation.
3. The acid/base titrations of Δ+PHS/V66K monitored by far-ultraviolet CD and by the intrinsic fluorescence of Trp-141 are shown in Fig. 4. The fluorescence-monitored titration of Δ+PHS is also included in this figure for comparison. Acid denaturation of Δ+PHS nuclease began at pH 2.5. The cooperative acid-unfolding transition of the Δ+PHS/V66K mutant occurred at pH ≤ 4.2, more than 1.5 pH units below the pK_a of Lys-66. Figure 4 also illustrates the excellent agreement between the acid-unfolding transition monitored by CD, by fluorescence, and by preferential H^+ binding to the acid denatured state. The latter curve is obtained by subtracting from the titration curve of Δ+PHS/V66K the H^+ titration curves of Δ+PHS and the titration curve of a single group with a pK_a of 5.7. All the different types of titration data show that the major acid-induced conformational transition began near pH 4.2, and ended near pH 3.4.
4. The pH dependence of 1D ^{1}H-NMR spectra of Δ+PHS/V66K is shown in Fig. 5. These spectra confirmed that Δ+PHS/V66K exists primarily in the native conformation at pH ≥ 4.2. The acid-induced conformational transition between pH 4.2 and 3.6 can be observed most

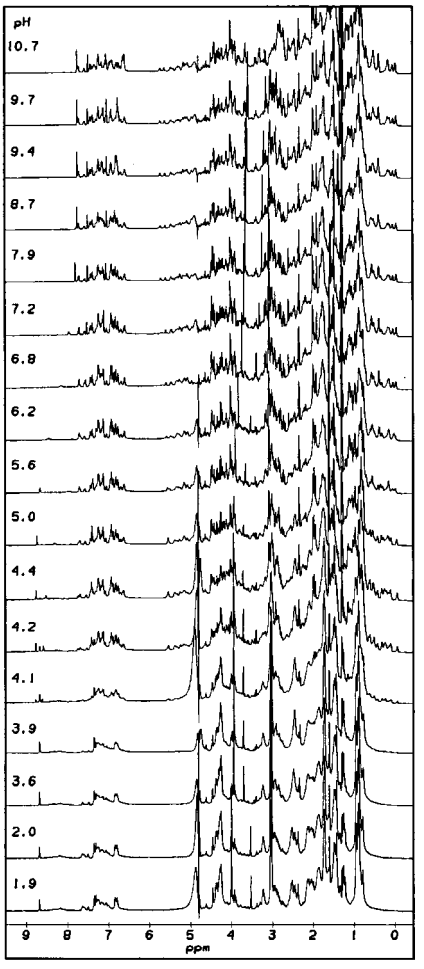

FIGURE 5 Acid/base titration of 1D ^{1}H-NMR spectra of Δ+PHS/V66K at 25°C in 100 mM KCl.

TABLE 1 pK_a Values of surface histidines and buried Lys-66 and Glu-66

	His-8*	His-46	His-121	His-124	Lys-66 or Glu-66†	Lys-66 or Glu-66‡
Wild type§	6.61 ± 0.07	5.94 ± 0.02	5.29 ± 0.04	5.81 ± 0.07		
PHS	6.53 ± 0.02	5.90 ± 0.02	5.31 ± 0.02			
Δ+PHS	6.50 ± 0.02		5.25 ± 0.04			
PHS/V66K	6.51 ± 0.05	6.38 ± 0.03	6.49 ± 0.17			6.35 ± 0.10¶
Δ+PHS/V66K	6.56 ± 0.01		5.38 ± 0.01		5.6 ± 0.01	5.76 ± 0.30
PHS/V66E					8.8 ± 0.10‖	8.5 ± 0.30‖

*Values determined by ^{1}H-NMR.
†Values determined potentiometrically.
‡Values determined from the pH dependence of $\Delta G^o_{H_2O}$.
§Errors are standard deviations from three separate experiments. All other errors in NMR-measured pK_a values are errors of the fit.
¶García-Moreno et al., 1997.
‖Dwyer et al., 2000.

dramatically in the pH-induced changes in the resonances in the aliphatic region (0–1 ppm) and in the aromatic region (6–9 ppm). The latter resonances, corresponding to the histidine residues, coalesced into a single resonance near 8.7 ppm at pH 3.6, suggesting that, in the acid-unfolded state, the histidine residues sampled, on average, identical microenvironments. The titration curves obtained by plotting the area under the upfield resonances of Val-74 against pH also paralleled the acid/base titration monitored spectroscopically or potentiometrically (data not shown).

5. Finally, the pK_a values of the surface histidines His-8 and His-121 are very similar in Δ+PHS, in Δ+PHS/V66K, and in the wild-type protein (see Table 1). This suggests that Δ+PHS/V66K is native-like down to pH 4. In contrast, the pK_a values of histidines in PHS/V66K are the same as the values for histidine in water, as expected, because the titration of the buried Lys-66 induces a substantial conformational transition (García-Moreno E. et al., 1997).

The experimental observations demonstrate unequivocally that the Δ+PHS/V66K mutant exists primarily in the fully folded, native conformation at pH values more than a full pH unit below the pK_a of Lys-66. This does not imply that local rearrangement or minor conformational changes do not occur upon ionization of the buried residues, but if structural changes do occur, they are invisible to the spectroscopic probes that were used. Note that, even if local rearrangements take place, the interpretation of ΔpK_a values in terms of dielectric properties of the protein is meaningful. The ΔpK_a can still be used to determine the highest value of ϵ_{in} needed to reproduce the pK_a values with a given computational method.

Surface ionizable groups do not sense the positive charge of Lys-66

Electrostatic interactions between surface ionizable groups and the buried Lys-66 could significantly influence the pK_a value of the buried group. Were this the case, some surface basic and acidic residues should exhibit more depressed pK_a values in the Δ+PHS/V66K mutant than in the Δ+PHS protein. The titration curves show no evidence of this. Once corrected to account for the potentiometric H^+ titration curve of Lys-66, the H^+ titration properties of Δ+PHS and Δ+PHS/V66K were nearly identical down to pH 4.2, where the acid unfolding transition of Δ+PHS/V66K begins (See Figs. 1 and 4). According to structure-based pK_a calculations discussed ahead, the pK_a of His-121 would have been depressed significantly in Δ+PHS/V66K if the electrostatic interactions between Lys-66 and His-121 were strong. Instead, the pK_a values of histidines listed in Table 1 show that His-121 titrated with almost identical pK_a values in Δ+PHS and in Δ+PHS/V66K. The slight shift in the pK_a of His-121 in these two proteins reflects our inability to collect the entire acid limit of the titration curve of this histidine because of the acid denaturation of the protein. The chemical shifts of His-121 in Δ+PHS/V66K and in Δ+PHS are identical down to the lowest pH in which the protein exists mainly in the native state. Overall, the data suggest that the electrostatic interactions between the buried Lys-66 and surface ionizable residues are negligible.

Meaning of dielectric constants in continuum models

It is of interest to identify the values of the protein dielectric constant, ϵ_{in}, needed to reproduce pK_a values quantitatively with a continuum model for structure-based pK_a calculations. To appreciate the significance of the values of ϵ_{in} thus resolved, it is necessary to review the meaning of ϵ_{in}.

The semi-macroscopic continuum model is based on the macroscopic model of Warwicker and Watson (1982), which treats the protein interior as a medium with low dielectric constant. However, this model also considers the microscopic features of the protein permanent dipoles (Warshel and Russell, 1984) by representing them explicitly in terms of partial charges (Klapper et al., 1986; Warshel et

al., 1989; Bashford and Karplus, 1990). When this model is used with a static structure to calculate the pK_a values of surface groups, ad hoc use of $\epsilon_{in} \approx 20$ is required to reproduce pK_a values (Antosiewicz et al., 1994). However, as demonstrated in the present study, high values of ϵ_{in} grossly underestimate the self-energies of buried groups; considerably lower values of ϵ_{in} are required to capture the pK_a values of buried groups consistently (Antosiewicz et al., 1994; Demchuk and Wade, 1996; Sham et al., 1997; Schutz and Warshel, 2001). Self-consistent calculation of pK_a values of surface and buried groups using a single value of ϵ_{in} is impossible with semi-macroscopic methods unless protein flexibility is taken into account explicitly. When conformational relaxation is treated explicitly, low ϵ_{in} can yield reasonable results (Langsetmo et al., 1991; Antosiewicz et al., 1994, 1996; You and Bashford, 1995; Alexov and Gunner, 1997; Zhou and Vijayakumar, 1997; Rabenstein et al., 1998; van Vlijmen et al., 1998; Havranek and Harbury, 1999; Scharnagl et al., 1999; Ullmann and Knapp, 1999), especially when the neutral and the ionized states of the group of interest are treated separately to capture contributions by the relaxation of local dipoles upon ionization (Langen et al., 1992; Yang et al., 1993; Alexov and Gunner, 1997; Sham et al., 1997; Zhou and Vijayakumar, 1997; Rabenstein and Knapp, 2001). In microscopic methods, such as the protein dipole–Langevin dipole (PDLD) method developed by Warshel and co-workers, the relaxation of protein dipoles has always been included explicitly (Warshel and Russell, 1984). Microscopic models are not yet fully convergent, thus a semi-macroscopic PDLD/S model (Warshel et al., 1989) was developed that uses a dielectric constant to account implicitly for energy contributions that do not converge completely in the fully microscopic simulations (Schutz and Warshel, 2001).

The appropriate choice of ϵ_{in} in semi-macroscopic continuum models is not obvious, as discussed previously by Warshel (Warshel and Russell, 1984; King et al., 1991). A single value of ϵ_{in} is not necessarily appropriate because the protein interior is highly heterogeneous and anisotropic; a single value implies that dielectric relaxation is the same in all proteins, and uniform throughout any one protein. This is unlikely (Demchuk and Wade, 1996; Sham et al., 1997; Simonson et al., 1999; Gunner and Alexov, 2000). ϵ_{in} need not be the same in the hydrophobic core, where electronic polarizability makes the dominant contribution, near the surface, where the reaction field from bulk water and flexibility of charged side chains are more dominant, and in intermediate regions, where reorganization of permanent dipoles are important (Simonson and Perahia, 1995; Simonson and Brooks, 1996). Furthermore, different dielectric constants are necessary to describe formally the two different components of the dielectric response upon ionization of a buried group: one to account for the static equilibrium charge distribution, and a higher value to account for relaxation (Krishtalik et al., 1997; Simonson et al., 1999). Similarly, different values of ϵ_{in} are needed to capture self-energies and coulombic energies (Warshel and Papazyan, 1998), although these could be captured by a single value of ϵ_{in} if contributions by protein relaxation were accounted for consistently and explicitly (Sham et al., 1997).

It is also useful to recognize that the value of ϵ_{in} used in a calculation depends on the level of physical detail represented explicitly in a model (Schutz and Warshel, 2001). In fully microscopic simulations, $\epsilon_{in} = 1$ because all contributions to dielectric relaxation in the protein–water system are treated explicitly. In calculations with continuum models ϵ_{in} is always >1. However, in these models ϵ_{in} is not strictly a dielectric constant. It is a scaling parameter meant to represent contributions that are not included explicitly in the model (Simonson et al., 1999; Schutz and Warshel, 2001). Implicit treatment of induced dipoles (electronic polarization) requires $\epsilon_{in} \approx 2$. When induced dipoles and protein relaxation (nuclear relaxation or reorientation of dipoles) are implicit, $\epsilon_{in} \approx 4$–10 should be used (Warshel et al., 1997; Rabenstein et al., 1998; Simonson et al., 1999). Even higher values of $\epsilon_{in} \geq 20$ are necessary to capture correctly pK_a values of surface residues. These high values of ϵ_{in} account implicitly for relaxation of permanent dipoles upon charging (Rabenstein et al., 1998; Sham et al., 1998). The essential point is that protein dielectric constants used in continuum models are not fundamental parameters. They are empirical parameters that need to be calibrated against microscopic simulations (Sham et al., 1998; Warshel and Papazyan, 1998; Simonson et al., 1999), or ideally against experimental data in carefully controlled situations, as in the present study.

Comparison of measured and calculated H^+ titration behavior of surface residues

To determine the range of values of ϵ_{in} needed to reproduce pK_a values, we focus first on the surface residues. The potentiometric H^+ titration curves of Δ+PHS nuclease and of the Δ+PHS/V66K mutant are compared with the curves calculated with the continuum method in Fig. 6. Calculated curves obtained with ϵ_{in} of 4, 10, and 20 are shown. As expected, the agreement between measured and calculated behavior was very poor with $\epsilon_{in} = 4$, and satisfactory with $\epsilon_{in} \geq 10$. The slight differences between the curves calculated with $\epsilon_{in} = 20$ and with $\epsilon_{in} = 10$ in the pH range 5.7–9.0 (Fig. 6 *B*) reflect differences in the state of ionization of the buried Lys-66, which titrates with a high pK_a when $\epsilon_{in} = 20$ and with a much lower one when $\epsilon_{in} = 10$. Comparison of calculated and measured titration behavior for Δ+PHS/V66K is only meaningful at pH $>$ 4.2. The divergence between the measured and calculated H^+ titration curves at pH $\leq$ 4.2 reflects preferential H^+ binding by the acid denatured form of Δ+PHS/V66K in the experimental curve. On the other hand, the divergence between measured and calculated H^+ titration curves of Δ+PHS

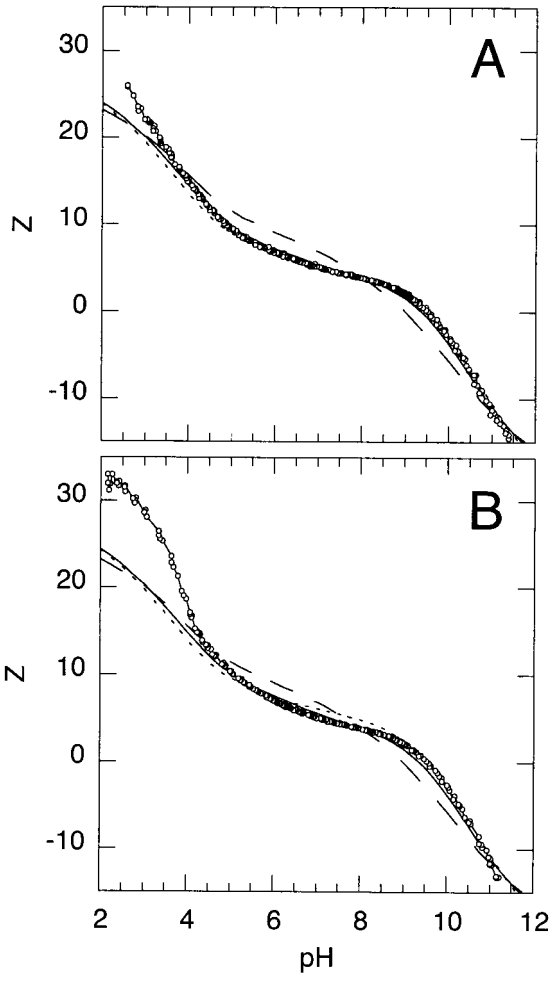

FIGURE 6 (*A*) pH Dependence of the net charge of Δ+PHS nuclease measured potentiometrically (*open circles*) and calculated using $\epsilon_{in} = 4$ (*dashed line*), 10 (*solid line*), and 20 (*dotted line*). All data were measured or calculated at 25°C in 100 mM KCl. The experimental data were shifted arbitrarily along the ordinate to superimpose them artificially with the data calculated with $\epsilon_{in} = 10$. (*B*) Same as in (*A*) but for Δ+PHS/V66K nuclease.

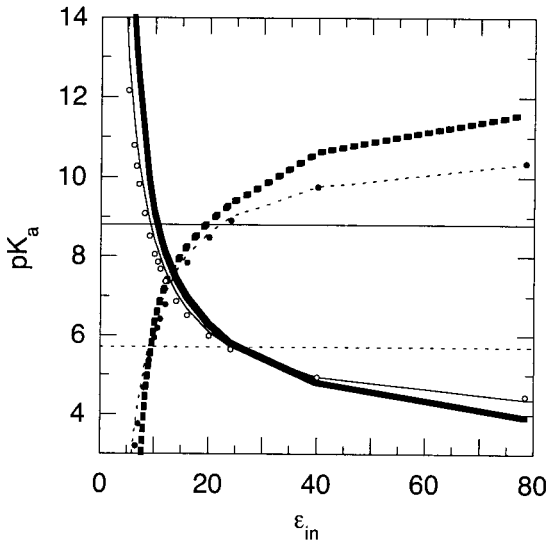

FIGURE 7 pK_a values of Lys-66 in Δ+PHS/V66K (*thick dashed*) and Glu-66 in PHS/V66E (*thick solid*), calculated as a function of ϵ_{in} with the semi-macroscopic methods based on finite-difference solution of the linearized Poisson–Boltzmann equation. The buried water molecules were not included explicitly in these calculations. Also shown are the Born energy (*open* and *closed circles*) calculated with the finite difference calculation, and the Born energy (*thin solid* and *dashed lines*) calculated with Eq. 3 in Dwyer et al. (2000). The thin horizontal solid lines identify the experimental pK_a values of Lys-66 (dashed) and Glu-66 (solid). Calculations and experimental data are at 25°C and 100 mM NaCl.

nuclease at low pH values is meaningful. It reflects inaccuracies in the calculated pK_a values of acidic residues not related to inherent problems with the algorithm, but to the use of a static structure under conditions of pH where considerable structural relaxation takes place (C. Fitch, S. Whitten and B. García-Moreno, in preparation).

Calculated pK_a values of the buried Lys-66 and Glu-66

Figure 7 shows pK_a values of Lys-66 and Glu-66 calculated as a function of ϵ_{in} with the continuum method using a static structure. The calculated pK_a values of Lys-66 and Glu-66 were only slightly dependent on ϵ_{in} when $\epsilon_{in} > 20$, but steeply dependent at lower values of ϵ_{in}. Calculations with $\epsilon_{in} = 4$, a value commonly used to represent the dielectric properties of the protein interior, failed dramatically to capture the experimental pK_a values. The empirical values of ϵ_{in} that best reproduced the experimental pK_a values of Glu-66 and Lys-66 were 10.5 and 9.5, respectively. Almost identical apparent dielectric constants were obtained by analysis of ΔpK_a with a simple Born formalism (García-Moreno E. et al., 1997; Dwyer et al., 2000), also shown in Fig. 7.

The dominant determinant of the pK_a values was the desolvation of the charged group when it is buried in the protein. This was established by dissection of the calculated pK_a values into energetic contributions from coulombic, Born, and background terms (Bashford and Karplus, 1990; Sham et al., 1997). The dependence of the Born energy on ϵ_{in} closely parallels that of the pK_a itself (Fig. 7). In contrast, the contributions to pK_a values from interactions with polar or surface charged residues were negligible when $\epsilon_{in} \geq 10$, consistent with the experimental observation that coulombic interactions between the buried Lys-66 or Glu-66 and surface ionizable residues are weak. The interactions between surface and buried ionizable groups become increasingly significant with $\epsilon_{in} \leq 10$. Those with polar atoms remain small even at low values of $\epsilon_{in} \approx 4$ because the buried charged group makes minimal contact with side chain or backbone polar atoms.

In general, $\epsilon_{in} = 20$ is the empirical value of choice that maximizes agreement between calculated and measured pK_a values of surface groups (Antosiewicz et al., 1994). The data in Fig. 6 show that this holds true for SNase. However, $\epsilon_{in} = 20$ is too high a value to capture the self-energies of Glu-66 and Lys-66 (Fig. 7). $\epsilon_{in} \approx 10$ is the empirical dielectric constant that captures pK_a values of buried groups at this location in SNase. Coincidentally, in the case of SNase, this value also captures the behavior of surface groups quantitatively (see Fig. 6). The empirical value $\epsilon_{in} = 10$ is unlikely to be of general use for estimation of pK_a values of buried groups. This high apparent polarizability probably reflects, at least partly, contributions by water penetration to the dielectric response of the protein that were not treated explicitly in the calculations, and it remains to be established that water penetration is a general mechanism of dielectric relaxation in proteins. Experimental studies are underway to determine empirically the values of ϵ_{in} required by this continuum method to capture the experimental pK_a values of groups buried at other locations in SNase and in other proteins.

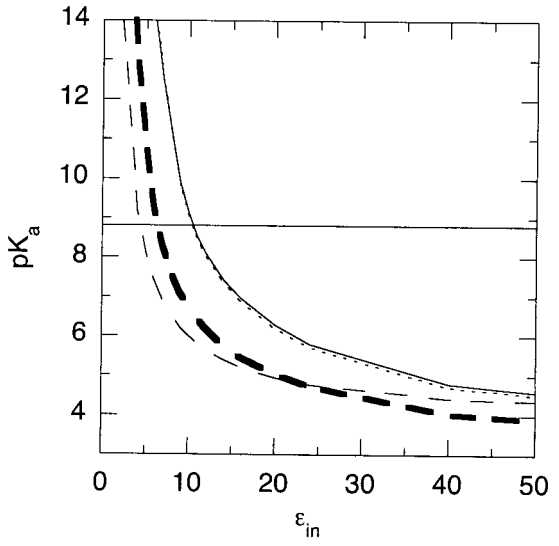

FIGURE 8 pK_a Values of Glu-66 in PHS/V66E calculated as a function of ϵ_{in} with buried water molecules omitted (*solid*) and with buried water molecules included after energy minimization of hydrogens with Glu-66 in the neutral state (*dotted*) or in the charged state and with coulombic interactions included (*thick dash*), or excluded (*thin dash*). The horizontal line identifies the experimental pK_a of Glu-66. Calculations and experimental data are at 25°C and 100 mM NaCl.

Influence of internal, site-bound water on pK_a values of the buried Glu-66

To evaluate contributions by buried water molecules to the pK_a value of Glu-66, a continuum calculation was performed in which some of the internal water molecules were treated explicitly, as done previously by others (Langen et al., 1992; Yang et al., 1993; Gibas and Subramaniam, 1996; Alexov and Gunner, 1999; Schutz and Warshel, 2001). Only four waters were treated explicitly, the two that are hydrogen bonded directly to the carboxyl oxygen atoms of Glu-66, and the two that connect these with bulk water (Dwyer et al., 2000). Results from these calculations are presented in Fig. 8. The buried water molecules had no effect on pK_a values when the system was energy minimized with Glu-66 in the neutral state. In contrast, when the minimization was performed with Glu-66 in the charged state, the buried water molecules had a considerable effect on the pK_a value. In these calculations, the experimental pK_a values were reproduced with $\epsilon_{in} = 6.4$. However, with ϵ_{in} in this range, the calculated coulombic interactions between the buried Glu-66 and surface-charged residues are exaggerated and too large to be consistent with the experimental observations. When the coulombic interactions between buried and surface ionizable residues were artificially turned off, the experimental pK_a of Glu-66 was reproduced with $\epsilon_{in} = 4.3$. When, in addition to the repositioning of hydrogen atoms, the water oxygen atoms were also allowed to reposition during the minimization, the pK_a values were reproduced with $\epsilon_{in} = 5.0$.

The pattern of hydration of Glu-66 present in crystallographic structures at −178°C need not represent the state of hydration in solution at 25°C. To assess how the value of ϵ_{in} that reproduced pK_a values depended on the number of water molecules that were treated explicitly, calculations were also performed with only a subset of the explicit internal water molecules included. The positions and orientation of the internal water molecules after minimization were largely insensitive to the number of crystallographic water molecules included in the minimization procedure. When only the most deeply buried water molecule was treated explicitly, and when coulombic interactions were omitted, $\epsilon_{in} = 7.4$ reproduced the experimental pK_a value. When the two most deeply buried water molecules that are directly hydrogen bonded to the carboxyl group of Glu-66 were included, the pK_a values were reproduced with $\epsilon_{in} = 5.4$. These calculations have two important implications. They show that the two innermost water molecules directly hydrogen bonded to the carboxyl are the ones responsible for the dramatic effect of internal water on the pK_a value. The value of $\epsilon_{in} = 7.4$, or more exactly, the fact that $\epsilon_{in} > 4$, further suggests that there might be structural reorganization concomitant with ionization of Glu-66, that is not captured implicitly in the calculations with a static structure. This was also suggested by previous calculations with semimicroscopic methods (Schutz and Warshel, 2001).

The data in Figs. 8 and 9 provide a clear example of how it is impossible to capture the behavior of surface and buried groups with a single value of ϵ_{in} in calculations with semimacroscopic methods using a static structure. The problem is inherent to calculations with continuum methods, in which contributions by protein relaxation are subsumed in

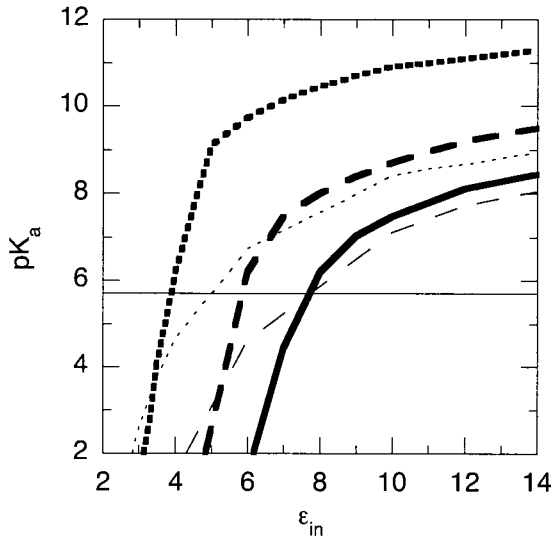

FIGURE 9 pK_a values of Lys-66 in PHS/V66K calculated as a function of ϵ_{in} with buried water molecules omitted (*thick solid*), with four buried water molecules included after energy minimization (allowing for movement of water molecules) with Lys-66 in the charged state, and with coulombic interactions included (*thick dotted*), or excluded (*thin dotted*). Also shown are results of calculations with only the two innermost buried waters included after minimization with Lys-66 in the charged state and coulombic energies included (*thick dashed*), or excluded (*thin dashed*). The horizontal line identifies the experimental pK_a of Lys-66. Calculations and experimental data are at 25°C and 100 mM NaCl.

ϵ_{in}, which need be neither uniform throughout the protein, nor the same for calculations of self-energies and coulombic energies. The problem can be avoided if, instead of using a single conformation in the calculations, the microscopic reorganization of the specific environments around the charges is accounted for explicitly. This can be done by the linear response approximation formulation of Warshel and coworkers, which requires averaging over the charge and uncharged configurations (Langen et al., 1992), and by a similar treatment in the more recent methods (Alexov and Gunner, 1997; van Vlijmen et al., 1998; Schutz and Warshel, 2001). These problems are also avoided in the method developed by Mehler and co-workers, which is based on the use of screened coulombic potentials coupled with a hydrophobicity parameter to account for variations in local microenvironments of ionizable groups (Mehler and Guarnieri, 1999).

Test of the hypothesis that Lys-66 in the buried state is hydrated

The only noteworthy difference between the crystallographic structures with Lys-66 and Glu-66 are the buried water molecules hydrogen bonded to the carboxyl of Glu-66. They are not present in two structures of V66K mutants of wild type and Δ+PHS nuclease, obtained at 25°C and −178°C, respectively. The absence of buried water molecules in the V66K structures is surprising because the ΔpK_a for Glu-66 and Lys-66 are virtually identical—these two groups experience equivalent net polarizability in the ionized state. The side chain of the buried Lys-66 is in an extremely hydrophobic environment, incompatible with the high apparent polarizability reflected in the ΔpK_a.

With the experimental data at hand, it is not possible to exclude the possibility that ionization of Glu-66 or Lys-66 is accompanied by local unfolding or minor restructuring of their local environment. Close examination of the structures and side chain rotamers suggests that side-chain extrusion toward bulk water would be very difficult in the case of Glu-66 except through local unfolding. The longer side chain of Lys-66 could reach the surface of the protein, but only by assuming a highly unfavorable conformation. In energy-minimization and molecular-dynamics simulations, the buried Lys-66 never abandons its buried position (Stites et al., 1991). In the absence of any direct, experimental evidence for structural conformational changes concomitant with ionization of the buried Lys-66, we entertain the hypothesis that the high polarizability reported by the pK_a of this group reflects contact with internal water similar to those seen in the structures with Glu-66. These buried waters could be transient, or disordered, and therefore crystallographically invisible. This is partly expected based on the observation that amines are weakly hydrated, especially compared to the strong hydration of carboxylic groups (Collins, 1997).

To determine how the pK_a of Lys-66 would be affected if it were in contact with internal water molecules, we performed calculations with a model of the structure of PHS/V66K, made by introducing an Lys at position 66 into the PHS/V66E structure with the conformation that Lys-66 has in Δ+PHS/V66K. The results are presented in Fig. 9. When the orientation of the buried water molecules was energy minimized with Lys-66 in the charged state, and when the coulombic interactions between buried and surface ionizable residues were included, the experimental pK_a value was reproduced with $\epsilon_{in} = 3.9$. When the coulombic interactions were omitted, $\epsilon_{in} = 5.0$ reproduced the pK_a values. Again, the two most deeply buried water molecules were the ones that influenced the pK_a of Lys-66 the most. The value of ϵ_{in} needed to reproduce the experimental pK_a increased toward 7.5 when only one of the innermost water molecules was included in the calculation.

Detailed views of the buried side chains of Glu-66 and Lys-66 and the positions and orientation of the water molecules minimized with the neutral and charged form of the buried group are shown in Fig. 10. The hydrogen-bonding patterns between the buried water molecules, the buried side chain, and backbone polar atoms are substantially different in the cases of Glu-66 and Lys-66. Despite these differences, the pK_a values of Glu-66 and Lys-66 were captured with nearly identical values of ϵ_{in}, in the

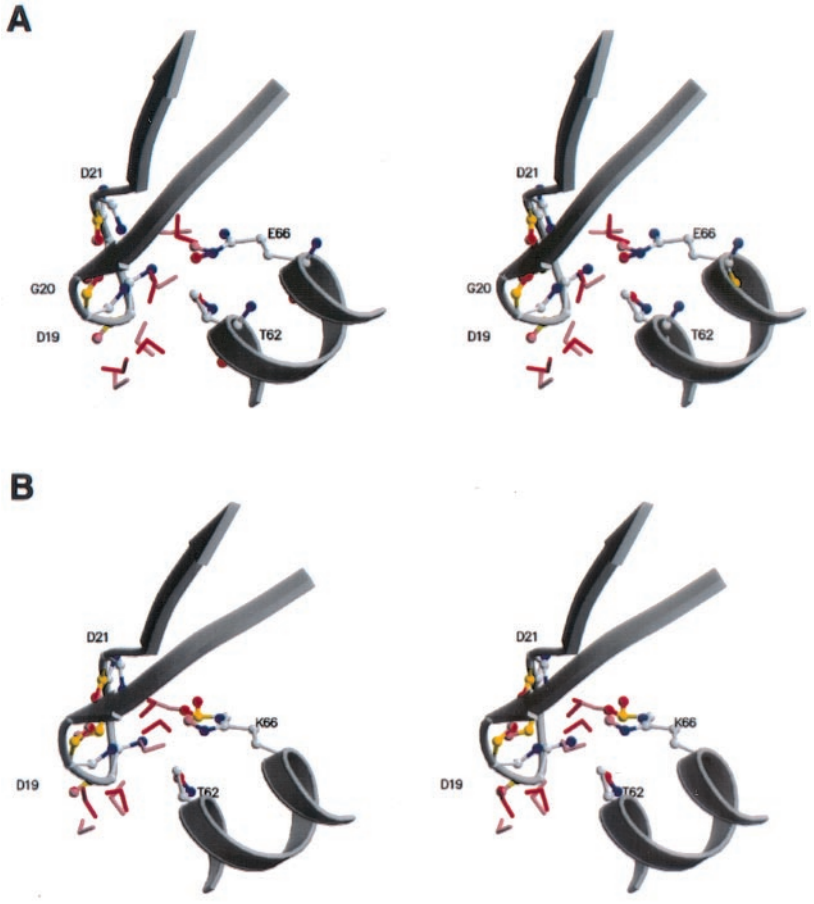

FIGURE 10 Microenvironments around (*A*) Glu-66 in PHS/V66E. Water molecules and some hydrogen ions are shown after minimization with Glu-66 in the neutral (*pink*) and charged (*red*) states. (*B*) Lys-66 in the artificial PHS/V66K with the side chain of Glu-66 superimposed for comparison. Shown are the position and orientation of water molecules after minimization with Glu-66 in the neutral state (*pink*), or with Lys-66 in the charged state (*red*). Images drawn with MOLSCRIPT and with Raster 3D (Kraulis; 1991; Merritt and Bacon, 1997).

range 4–5 when the water molecules were allowed to relax. This figure shows that, in the Lys-66 mutant, there is a sufficiently large volume to accommodate the water molecules. However, the pentagonal structures formed by the carboxylic moiety of Glu-66, the backbone polar atoms, and the water molecules, cannot be formed with Lys-66. This might be another reason why the internal waters are more disordered in the presence of Lys-66, and therefore crystallographically invisible.

In calculations with low values of ϵ_{in}, the details of the calculations matter greatly: the manner in which explicit water molecules are treated, the specific procedure for energy minimization, and the choice of charge set used in the calculations to represent permanent dipoles can have significant effects. Even for surface residues, the agreement between experimental and calculated pK_a values in calculations with $\epsilon_{in} \approx 4$ can be improved simply by redistributing charge on the ionizable side chain (Antosiewicz et al., 1996). More sophisticated treatment of multiple conformers and different placement of hydrogen atoms in the region around the buried residues is warranted when $\epsilon_{in} \approx 4$ (Alexov and Gunner, 1997). These issues will be addressed in the future, when additional experimental pK_a values of buried residues are available to critically assess the performance of the computational models. However, the conclusions from the calculations in Figs. 8 and 9, regarding the important role of buried water molecules in determining pK_a values of buried groups, are independent of the details of the calculations. They demonstrate that internal water molecules can contribute significantly to the high apparent polarizability reported by Glu-66. They support the hypothesis that the buried Lys-66 interacts with internal waters. They illustrate the profound effects that water penetration can have on the electrostatic properties of ionizable groups buried in the protein interior or at interfaces between macromolecules. One or two buried water molecules in the vicinity of a buried Lys or Glu can modulate its pK_a within the physiologically relevant range of pH. According to these calculations, internal water molecules in proteins can be

only slightly less effective than bulk water in solvating buried groups and in stabilizing charge.

Structural relaxation upon charging of the buried ionizable residues

To interpret the meaning of the ϵ_{in} values obtained from the different simulations shown in Figs. 8 and 9, it is useful to remember that the equilibrium dielectric constants of dried proteins and peptides measured experimentally are in the range 2–4 (Harvey and Hoekstra, 1972). In the limit of extreme dehydration, dried proteins are presumably still folded in native-like conformations, rigid, uncharged, with all polar groups hydrogen bonded among themselves (Rupley and Careri, 1991). Under these conditions, and in the high-frequency limit, the static dielectric constant is actually closer to 2. Therefore, $\epsilon_{in} \approx 2$ reflects mainly electronic polarizability. $\epsilon_{in} \approx 4$ is thought to include contributions by relaxation of permanent dipoles in addition to electronic polarizability.

In the calculations in which four water molecules were treated explicitly, $\epsilon_{in} \approx 4$–5 captured pK_a values of both Lys-66 and Glu-66 with a single conformation. This suggests that, if the pattern of hydration observed crystallographically is the one populated in solution, then the buried groups can ionize without triggering any significant structural relaxation in SNase beyond the fluctuation of permanent dipoles already implicit in $\epsilon_{in} = 4$–5. This is consistent with the experimental data showing that SNase is folded and indistinguishable from the native protein at pH values below the pK_a of Lys-66 and above the pK_a of Glu-66. The implications are that SNase behaves as a rigid body that minimizes the energetic consequences of burial and ionization of a polar group in a highly nonpolar environment by allowing the penetration of water into the core, rather than by undergoing significant structural reorganization. The response is different from that expected from regions of proteins that have evolved to solvate buried charges. In the active sites of enzymes, for example, the dominant mechanisms of dielectric relaxation might involve a more significant reorientation of polar groups (Warshel, 1987). In these cases, the values of ϵ_{in} used to represent protein relaxation are higher, ranging from 4 to 8 (Sham et al., 1997; Simonson et al., 1999; Schutz and Warshel, 2001). $\epsilon_{in} \approx 4$ are more consistent with the microscopic fluctuations in the core of several proteins studied by molecular-dynamics simulations (Smith et al., 1993; Simonson and Brooks, 1996; Simonson and Perahia, 1996), and with values of ϵ_{in} found to reproduce reorganizational energies in electron transfer systems (Muegge et al., 1997; Sharp, 1998).

One reason why the significance of $\epsilon_{in} = 4$–5 should not be over-interpreted is that the relaxation of the water molecules in the calculations in Figs. 8 and 9 was handled through an energy-minimization procedure, instead of through more physically realistic Monte Carlo or molecular-dynamics simulations. The energy-minimized structures bias the orientation of water molecules toward the energetically most favorable state relative to the charged group. The natural result of this procedure is to minimize the values of ϵ_{in} needed to capture the experimental pK_a values. More explicit simulations are underway to determine whether the same effect could be achieved if configurational averaging over neutral and ionized states based on molecular dynamics were used to capture the reorganization of water molecules and protein dipoles explicitly.

The values of $\epsilon_{in} \approx 7.5$ obtained when the pK_a values are analyzed with only the one or two innermost water molecules treated explicitly suggest that conformational reorganization concomitant with ionization of the buried group can occur. Conformational changes were not detected by a variety of spectroscopic probes. Therefore, if they occur, they must be minor, and local rather than global. They might involve local and transient unfolding to expose the charged Lys-66 or Glu-66 to water, or a slight change in the interactions between the helix where position 66 is found and the rest of the protein, to enhance hydration of the charged group.

CONCLUSIONS

When Lys or Glu are buried at position 66 in SNase, the equilibrium between the ionized and the neutral states shifts substantially in favor of the neutral state, thus the pK_a values of acidic residues are elevated, and those of basic residues are depressed relative to pK_a values in water. The dominant determinant of the pK_a values of these buried residues is the difference in the Born energy of the charged species in bulk water and in the protein interior. Although the pK_a shifts of Lys-66 and Glu-66 are among the largest ever measured, the remarkable aspect is that they are actually very modest compared to the energetic cost of transferring a charge from water to a nonpolar environment. In SNase, water penetration can apparently contribute significantly to the stabilization of ionizable and charged groups in the protein interior. Buried water molecules can ameliorate the energetic penalty of removal of a polar side chain from bulk water, and they can reduce the magnitude of the shift in pK_a value that a buried group would experience. Modulation of pK_a values of buried groups in the physiological range of pH through interactions with internal water molecules is a recurring motif encountered in many membrane proteins involved in H^+ and e^- transport, and in active sites of enzymes.

Dielectric constants used in continuum methods to describe polarizability in the protein interior are empirical parameters meant to account implicitly for contributions not considered explicitly in computational models (Schutz and Warshel, 2001). These parameters need to be calibrated against microscopic calculations or against experimental data. In the case of SNase, the pK_a value of residues buried

at position 66 were reproduced with a continuum model when $\epsilon_{in} \approx 10$. This value of ϵ_{in} is high because it reflects significant contributions by water penetration and minor conformational reorganization that are not handled explicitly in the calculations. When four internal water molecules were treated explicitly, the value of ϵ_{in} that reproduced pK_a values of buried residues dropped to 4–5. This should not be construed as evidence that $\epsilon_{in} = 4–5$ is the true macroscopic dielectric constant of SNase in particular, or of proteins in general. It should also not be assumed that this value of ϵ_{in} is relevant for calculations of pKa values of buried residues with these methods in other proteins or even at other sites in SNase. The spatial dependence of ϵ_{in} in the interior of proteins remains unknown.

The consequence of treating the buried, site-bound water molecules explicitly was to depress the value of ϵ_{in} used in the calculation because, in general, the less implicit the model, the lower the dielectric constant required. The value of $\epsilon_{in} \approx 4–5$ required to reproduce pK_a values when all internal waters were treated explicitly implies that the ionization of these buried residues does not result in a significant conformational reorganization. However, when fewer water molecules were treated explicitly, this value of ϵ_{in} increases to values near 7.5. This means that, if the buried ionizable groups are less hydrated than suggested by the crystallographic structures, then conformational reorganization must take place upon ionization of the buried residues.

The meaningful interpretation of ΔpK_a in terms of ϵ_{in} in SNase was possible because position 66 is unique in several respects. The ionizable moieties of Glu-66 and Lys-66 sit in one of the most hydrophobic environments in which buried ionizable groups have ever been found (Mehler et al., 2002). There are no backbone or side-chain polar groups nearby that could affect the pK_a values significantly. The ionizable moieties of Lys-66 and Glu-66 are also buried too deeply to sense the reaction field of bulk water, and they are too far from surface charges to be affected through coulombic interactions. The response of SNase as a rigid body to the ionization of a group buried in its hydrophobic core is also noteworthy. Proteins that have evolved to solvate buried charges, for example, at active sites, are expected to be more pliable than SNase and might require $\epsilon_{in} > 4$ to capture the energetics of ionization of buried groups, depending on the level of relaxation included explicitly in the calculations.

Without the extensive experimental constraints available for these SNase mutants, it would have been impossible to reach many of the conclusions of this study. For example, interactions between the buried and surface ionizable groups were excluded arbitrarily in some of the calculations because the experimental evidence indicated that these interactions are negligible. The evidence that water penetration played a significant role was based on direct crystallographic observation of water penetration; it is not yet obvious that the presence of buried water molecules could have been predicted from physical principles. The experimental demonstration that the structural consequences of the ionization of buried groups are minimal was also necessary for the interpretation of the values of ϵ_{in} that reproduce the experimental data.

The thermodynamic data and the crystallographic structures of mutants with Lys-66 and Glu-66 raise several interesting and challenging problems related to water penetration in proteins. The data suggest that water penetration can play a significant role in the stabilization of charge in the protein interior. They also suggest that crystallographic structures are not necessarily dependable sources of information about patterns of hydration of buried groups. Without the structure of mutants with Glu-66 to identify the hydration motif, any attempts based solely on the structure with Lys-66 to elucidate microscopic origins of polarizability in the protein interior would have failed to include the possible significant contributions of transient, buried water molecules in the hydrophobic core. The physical origins of permittivity in the protein interior would have been misinterpreted. To improve the accuracy and utility of structure-based calculations of electrostatic energy in proteins, methods will have to be developed to identify water-binding sites, to calculate the occupancy of the binding sites, and to calculate conformational relaxation of internal water molecules (Warshel and Papazyan, 1998).

SNase appears to be unable to retain a charged group in a nonpolar environment without undergoing at least local rearrangement or without water penetration, as proposed originally by Warshel for proteins in general (Warshel, 1981; Warshel and Papazyan, 1998). The extent to which water penetration occurs in other proteins or in other locations in SNase is unknown at this time. The magnetic relaxation dispersion studies by Halle and Denisov suggest that water penetration is common, and that internal water molecules exchange rapidly with bulk water (Denisov and Halle, 1996; Denisov et al., 1997). Water penetration has also been observed and characterized in molecular-dynamics simulations (García and Hummer, 2000). Given the significant consequences of internal water molecules on pK_a values of buried groups, it will be necessary to improve our understanding of water penetration in proteins and of properties of internal water molecules, to elucidate structural origins of function in many key biochemical systems.

We gratefully acknowledge Prof. Juliette Lecomte (Pennsylvania State University) and Dr. Charles Long (The Johns Hopkins Nuclear Magnetic Resonance Facility) for technical advice on ^{1}H-NMR experiments, Prof. Andrew McCammon (University of California, San Diego) for access to the University of Houston Brownian Dynamics simulation package, and Ms. Mary Stahley (The Johns Hopkins University) for performing some of the stability measurements.

This work was supported by National Science Foundation grants MCB-9600991 to B.G.-M.E., and MCB-9982967 to E.E.L.

REFERENCES

Alexandrescu, A. T., D. A. Mills, E. L. Ulrich, M. Chinami, and J. L. Markley. 1988. NMR assignments of the 4 histidines of staphylococcal nuclease in native and denatured states. *Biochemistry*. 27:2158–2165.

Alexandrescu, A. T., E. L. Ulrich, and J. L. Markley. 1989. H-1-Nmr evidence for 3 interconverting forms of staphylococcal nuclease—effects of mutations and solution conditions on their distribution. *Biochemistry*. 28:204–211.

Alexov, E. G., and M. R. Gunner. 1999. Calculated protein and proton motions coupled to electron transfer: electron transfer from Q_A- to Q_B in bacterial photosynthetic reaction centers. *Biochemistry*. 38:8253–8270.

Alexov, E. G., and M. R. Gunner. 1997. Incorporating protein conformational flexibility into the calculation of pH-dependent protein properties. *Biophys. J.* 74:2075–2093.

Antosiewicz, J., J. A. McCammon, and M. K. Gilson. 1994. Prediction of pH-dependent properties of proteins. *J. Mol. Biol.* 238:415–436.

Antosiewicz, J., A. J. McCammon, and M. K. Gilson. 1996. The determinants of pK_as in proteins. *Biochemistry*. 35:7819–7833.

Bashford, D., and M. Karplus. 1990. pK_a's of ionizable groups in proteins: atomic detail from a continuum electrostatic model. *Biochemistry*. 29: 10219–10225.

Bhattacharya, S., and J. T. J. Lecomte. 1997. Temperature dependence of histidine ionization constants in myoglobin. *Biophys. J.* 73:3241–3256.

Cocco, M. J., Y. H. Kao, A. T. Phillips, and J. T. J. Lecomte. 1992. Structural comparison of apomyoglobin and metaquomyoglobin: pH titration of histidines by NMR spectroscopy. *Biochemistry*. 31: 6481–6491.

Collins, K. 1997. Charge density-dependent strength of hydration and biological structure. *Biophys. J.* 72:65–74.

Davis, M. E., J. D. Madura, B. A. Luty, and J. A. McCammon. 1991. Electrostatics and diffusion of molecules in solution—simulations with the University of Houston Brownian Dynamics program. *Comput. Phys. Commun.* 62:187–197.

Del Buono, G. S., F. E. Figueirido, and R. M. Levy. 1994. Intrinsic pK_as of ionizable residues in proteins: an explicit solvent calculation for lysozyme. *Proteins Struct. Funct. Genet.* 20:85–97.

Demchuk, E., and R. C. Wade. 1996. Improving the continuum dielectric approach to calculating pK_as of ionizable groups in proteins. *J. Phys. Chem.* 100:17373–17387.

Denisov, V. P., and B. Halle. 1996. Protein hydration dynamics in aqueous solution. *Faraday Discuss.* 193:227–244.

Denisov, V. P., K. Venu, J. Peters, H. D. Horlein, and B. Halle. 1997. Orientational disorder and entropy of water in protein cavities. *J. Phys. Chem. B* 101:9380–9389.

Dwyer, J., A. Gittis, D. Karp, E. Lattman, D. Spencer, W. Stites, and B. García-Moreno E. 2000. High apparent dielectric constants in the interior of a protein reflect water penetration. *Biophys. J.* 79:1610–1620.

Evans, P. A., R. A. Kautz, R. O. Fox, and C. M. Dobson. 1989. A magnetization-transfer nuclear magnetic-resonance study of the folding of staphylococcal nuclease. *Biochemistry*. 28:362–370.

Fox, R. O., P. A. Evans, and C. M. Dobson. 1986. Multiple conformations of a protein demonstrated by magnetization transfer NMR-spectroscopy. *Nature*. 320:192–194.

García, A. E., and G. Hummer. 2000. Water penetration and escape in proteins. *Proteins Struct. Funct. Genet.* 38:261–272.

García-Moreno E., B., J. Dwyer, A. Gittis, E. Lattman, D. Spencer, and W. Stites. 1997. Experimental measurement of the effective dielectric in the hydrophobic core of a protein. *Biophys. Chem.* 64:211–224.

Gibas, C. J., and S. Subramaniam. 1996. Explicit solvent models in protein pK_a calculations. *Biophys. J.* 71:138–147.

Gilson, M. K. 1993. Multiple-site titration and molecular modeling: two rapid methods for computing energies and forces for ionizable groups in proteins. *Proteins Struct. Funct. Genet.* 15:266–282.

Glasoe, P. K., and F. A. Long. 1960. Use of glass electrodes to measure acidities in deuterium oxide. *J. Phys. Chem.* 64:188–190.

Gunner, M., and E. Alexov. 2000. A pragmatic approach to structure based calculation of coupled proton and electron transfer in proteins. *Biochim. Biophys. Acta.* 1458:63–87.

Harvey, S. C., and P. Hoekstra. 1972. Dielectric relaxation spectra of water adsorbed on lysozyme. *J. Phys. Chem.* 76:2987–2994.

Havranek, J. J., and P. B. Harbury. 1999. Tanford-Kirkwood electrostatics for protein modeling. *Proc. Natl. Acad. Sci. U.S.A.* 96:11145–11150.

Hynes, T. T., and R. O. Fox. 1991. The crystal structure of staphylococcal nuclease refined at 1.7 Å resolution. *Proteins Struct. Funct. Genet.* 10:92–105.

Jorgensen, W. L., J. Chandrasekhar, J. D. Madura, R. W. Impey, and M. L. Klein. 1983. Comparison of simple potential functions for simulating liquid water. *J. Chem. Phys.* 79:926–935.

Jorgensen, W. L., and J. Tirado-Rives. 1988. The OPLS potential functions for proteins. Energy minimizations for crystals of cyclic peptides and crambin. *J. Am. Chem. Soc.* 110:1657–1666.

Kao, Y.-H., Fitch, C. A., Bhattacharya, S., Sarkisian, C. J., Lecomte, J. T. J., and García-Moreno, E., B. 2000. Salt Effects on Ionization Equilibria of Histidines in Myoglobin. *Biophys. J.* 79:1637–1654.

King, G., F. S. Lee, and A. Warshel. 1991. Microscopic simulations of marcroscopic dielectric-constants of solvated proteins. *J. Chem. Phys.* 95:4366–4377.

Klapper, I., R. Hagstrom, R. Fine, K. Sharp, and B. Honig. 1986. Focussing of electric fields in the active site of Cu-Zn superoxide dismutase: effects of ionic strength and amino-acid modification. *Proteins Struct. Funct. Genet.* 1:47–59.

Krishtalik, L. I., A. M. Kuznetsov, and E. L. Mertz. 1997. Electrostatics of proteins: description in terms of two dielectric constants simultaneously. *Proteins Struct. Funct. Genet.* 28:174–182.

Langen, R., G. M. Jensen, U. Jacob, P. O. Stephens, and A. Warshel. 1992. Protein control of iron-sulfur cluster redox potentials. *J. Biol. Chem.* 267:25625–25627.

Langsetmo, K., J. Fuchs, C. Woodward, and K. Sharp. 1991. Linkage of thioredoxin stability to titration of ionizable groups with perturbed pK_a. *Biochemistry*. 30:7609–7614.

Lecomte, J. T. J., and M. J. Cocco. 1990. Structural features of the protoporphyrin-apomyoglobin complex: a proton NMR spectroscopy study. *Biochemistry*. 29:11057–11067.

Li, N. C., P. Tang, and R. Mathur. 1961. Deuterium isotope effects on dissociation constants and formation constants. *J. Phys. Chem.* 65:1074-1076.

Loll, P. J., and E. E. Lattman. 1989. The crystal structure of the ternary complex of staphylococcal nuclease, Ca^{2+}, and the inhibitor pdTp, refined at 1.65 A. *Proteins Struct. Funct. Genet.* 5:183–201.

Markley, J. 1975. Observation of histidine residues in proteins by means of nuclear magnetic resonance spectroscopy. *Acc. Chem. Res.* 8:70–80.

Martin, M. L., G. J. Martin, and J.-J. Delpuech. 1980. Practical NMR Spectroscopy. Heyden, Philadelphia, PA.

Matthew, J. B., F. R. N. Gurd, B. García-Moreno E., M. A. Flanagan, K. L. March, and S. J. Shire. 1985. pH-Dependent properties in proteins. *CRC Crit. Rev. Biochem.* 18:91–197.

Mehler, E. L., M. Fuxreiter, I. Simon, and B. Barcía-Moreno E. 2002. The role of hydrophobic microenvironments in modulating pK_a shifts in proteins. *Proteins Struct. Funct. Genet.* In press.

Mehler, E. L., and F. Guarnieri. 1999. A self-consistent, microenvironment modulated screened coulomb potential approximation to calculate pH-dependent electrostatic effects in proteins. *Biophys. J.* 75:3–22.

Muegge, I., P. X. Qi, A. J. Wand, Z. T. Chu, and A. Warshel. 1997. The reorganization energy of cytochrome *c* revisited. *J. Phys. Chem. B.* 101: 825–836.

Neria, E., S. Fischer, and M. Karplus. 1996. Simulation of activation free energies in molecular systems. *J. Chem. Phys.* 105:1902–1921.

Rabenstein, B., and E. W. Knapp. 2001. Calculated pH-dependent population and protonation of carbon-monoxy-myoglobin conformers. *Biophys. J.* 80:1141–1150.

Rabenstein, B., G. M. Ullmann, and E. W. Knapp. 1998. Calculation of protonation patterns in proteins with structural relaxation and molecular

ensembles—application to the photosynthetic reaction center. *Eur. Biophys. J.* 27:626–637.

Rupley, J. A., and G. Careri. 1991. Protein hydration and function. *Adv. Prot. Chem.* 41:37–172.

Scharnagl, C., R. Raupp-Kossmann, and S. F. Fischer. 1999. Molecular basis for pH sensitivity and proton transfer in green fluorescent protein: protonation and conformational substates from electrostatic calculations. *Biophys. J.* 77:1839–1857.

Schutz, C. N., and A. Warshel. 2001. What are the dielectric "constants" of proteins and how to validate electrostatic models? *Proteins Struct. Funct. Genet.* 44:400–417.

Sham, Y. Y., Z. T. Chu, and A. Warshel. 1997. Consistent calculations of pK_a's of ionizable residues in proteins: semi-microscopic and microscopic approaches. *J. Phys. Chem. B.* 101:4458–4472.

Sham, Y. Y., I. Muegge, and A. Warshel. 1998. The effect of protein relaxation on charge–charge interactions and dielectric constants of proteins. *Biophys. J.* 74:1744–1753.

Sharp, K. 1998. Calculation of electron transfer reorganization energies using the finite difference Poisson–Boltzmann model. *Biophys. J.* 74: 1241–1250.

Shortle, D., and A. Meeker. 1986. Mutant forms of staphylococcal nuclease with altered patterns of guanidine hydrochloride and urea denaturation. *Proteins Struct. Funct. Genet.* 1:81–89.

Simonson, T., G. Archontis, and M. Karplus. 1999. A Poisson–Boltzmann study of charge insertion in an enzyme active site: the effect of dielectric relaxation. *J. Phys. Chem. B.* 103:6142–6156.

Simonson, T., and C. L. Brooks, III. 1996. Charge screening and the dielectric constant of proteins: insights from molecular dynamics. *J. Am. Chem. Soc.* 118:8452–8458.

Simonson, T., and D. Perahia. 1995. Microscopic dielectric properties of cytochrome *c* from molecular dynamics simulations in aqueous solution. *J. Am. Chem. Soc.* 117:7987–8000.

Simonson, T., and D. Perahia. 1996. Polar fluctuations in proteins: molecular-dynamic studies of cytochrome *c* in aqueous solution. *Faraday Discuss.* 103:71–90.

Smith, P. E., R. M. Brunne, A. E. Mark, and W. F. van Gunsteren. 1993. Dielectric properties of trypsin inhibitor and lysozyme calculated from molecular dynamics simulations. *J. Phys. Chem.* 97:2009–2014.

Stites, W. E., A. G. Gittis, E. E. Lattman, and D. Shortle. 1991. In a staphylococcal nuclease mutant the side-chain of a lysine replacing valine 66 is fully buried in the hydrophobic core. *J. Mol. Biol.* 221:7–14.

Ullmann, G. M., and E. W. Knapp. 1999. Electrostatic models for computing protonation and redox equilibria in proteins. *Eur. Biophys. J.* 28:533–551.

van Vlijmen, H. W. T., M. Schaefer, and M. Karplus. 1998. Improving the accuracy of protein pK_a calculations: conformational averaging versus the average structure. *Proteins Struct. Funct. Genet.* 33:145–158.

Warshel, A. 1981. Calculations of enzymatic-reactions—calculations of pK_a, proton-transfer reactions, and general acid catalysis reactions in enzymes. *Biochemistry.* 20:3167–3177.

Warshel, A. 1987. What about protein polarity? *Nature.* 330:15–16.

Warshel, A., G. Naray Szabo, F. Sussman, and J. K. Hwang. 1989. How do serine proteases really work? *Biochemistry.* 28:3629–3637.

Warshel, A., and A. Papazyan. 1998. Electrostatic effects in macromolecules: fundamental concepts and practical modeling. *Curr. Opin. Struct. Biol.* 8:211–217.

Warshel, A., A. Papazyan, and I. Muegge. 1997. Microscopic and semimacroscopic redox calculations: what can and cannot be learned from continuum models. *J. Biol. Inorg. Chem.* 2:143–152.

Warshel, A., and S. T. Russell. 1984. Calculations of electrostatic interactions in biological-systems and in solutions. *Q. Rev. Biophys.* 17: 283–422.

Warwicker, J., and H. C. Watson. 1982. Calculation of the electric potential in the active site cleft due to *α-helix dipoles. J. Mol. Biol.* 157:671–679.

Whitten, S. T., and B. García-Moreno E. 2000. pH Dependence of stability of staphylococcal nuclease: evidence of substantial electrostatic interactions in the denatured state. *Biochemistry.* 39:14292–14304.

Wishart, D. S., C. G. Bigam, J. Yao, F. Abildgaard, H. J. Dyson, E. Oldfield, J. L. Markley, and B. D. Sykes. 1995. ^{1}H, ^{13}C and ^{15}N chemical shift referencing in biomolecular NMR. *J. Biomol. NMR.* 6:135–140.

Yang, A.-S., M. R. Gunner, R. Sampogna, K. Sharp, and B. Honig. 1993. On the calculation of pK_a s in proteins. *Proteins Struct. Funct. Genet.* 15:252–265.

You, T., and D. Bashford. 1995. Conformation and hydrogen ion titration of proteins: a continuum electrostatic model with conformational flexibility. *Biophys. J.* 69:1721–1733.

Zhou, H.-X., and M. Vijayakumar. 1997. Modeling of protein conformational fluctuations in pK_a predictions. *J. Mol. Biol.* 267:1002–1011.